Journal of Brilliant Engineering 2 (2026) 41109

Brilliant Engineering

journal home: www.acapublishing.com/journals/4/ben

Research Article

Concrete's Role in Plain Concrete Deep Beams' Shear Strength

Nwzad Abduljabbar Abdulla*,[1]

[1]*University of Salahaddin, Kerkuk road, Erbil, Iraq*

Keywords

a/h ratio,
Shear models,
Plain concrete,
Shear strength,
Simplified STM,
Small-scaled deep beam.

Abstract

This experimental study assessed the ultimate shear capacity of fifteen small-scale deep beams. To isolate the contribution of concrete tensile and compressive mechanisms to shear resistance in the absence of reinforcement, all the beams were made only from plain concrete and subjected to flexural three- and four-point loading. The main variables included the type of load, and the ratio of shear span to overall depth (a/h). Test results showed that as the a/h ratio decreased, the experimental shear's variability increased. The shear capacity as the absolute peak of tested specimens was most effectively increased when the a/h ratio was 1. Strength improved less when the a/h ratio was increased over this threshold. Moreover, only thirty-five models among the existing shear equations for normal reinforced concrete beams were suitable to predict the shear capacity of small-sized plain concrete deep beams. The majority of the thirty-five shear models' predictions are conservative. Nevertheless, the remaining models produced predictions that were unsafe. All the 35 shear models failed to capture the experimental behavior of group A-3 and reflect the effect of keeping a/h constant on the predicted shear values. Finally, a simplified strut-and-tie-based shear model (STM)is proposed. Moreover, the predictive STM expression was modified, calibrated for the tested beam range in group three. The accuracy of the proposed and modified STM model was verified by comparison with experimental testing results, yielding better predictions compared with the existing 35 shear models with an absolute average error value of only 12.9%.

1. Introduction

Shear failure is generally more catastrophic than flexural failure and one of the main causes of destruction of buildings during a natural disaster [1]. Researchers have extensively studied the shear behavior of simply supported reinforced concrete beams [2], deep beams (DB) [3], and short-span beams [4] in the past. The behavior of a deep beam under load is influenced by the effect of the force-transferring mechanism [5]. For steel reinforced deep beams, the strut and tie method (STM) evolved as a design tool for structural components, and it gives a rational approach whereby simplified truss models are used to represent complex structural components. The struts are intercepted by the stirrups [6].

Plain concrete specimens are permitted only in certain cases according to ACI code [7]. Ex. Members such as deep foundation, where the unsupported height does not exceed three times the least horizontal dimension and there is no requirement for resisting lateral loads. This is mandated by the code in order to avoid the tension-controlled brittle failure, which is the case in unreinforced beams. The structural integrity of structural plain concrete is affected by variables such as specimen size, concrete strength, and other properties of concrete [7]. Small-scale beams have been previously used in experimental studies. The use of small-scale beams is advantageous due to the ease of handling. Moreover, it is more representative to assess the fiber reinforced concrete specimens to be adopted in low height structural elements such as concrete sheets and thin slabs [8]. Plain concrete specimens have inferior resistance to cracking and its propagation when compared with steel fiber reinforced concrete specimens [9]. The developed shear forces minimize the flexural capacity of the concrete specimens. The shear strength of plain concrete beams was 111% lower than that for steel fiber beams, and this was ascribed to the lower tensile stress transfer capacity of plain concrete specimens [10]. The three parameters—aggregate interlock, shear force in the compression zone, and dowel action—are dependent on concrete strength [11]. The stress-displacement relationships proposed in research [12] were proved to be applicable to existing data for both plain concrete and reinforced concrete specimens [13]. The uncracked section assumption is assumed for the shear requirements of unreinforced concrete. Shear failure becomes imminent when the tensile stress in the specimen is equal to the tensile strength of the concrete. Most of the tensile stresses are shear-based. Against tension failure, the ACI code [7] imposes safety measures in order to limit the permissible shear. Generally, very few studies examined the shear behavior of plain concrete beams. Four plain DB (designated as duplicate specimens 1 and 2) with circular openings located in the shear span and midspan were examined in an experimental and analytical study. The dimensions of the deep beams were 200 mm in width, 480 mm in depth, and 820 mm in length and were all tested under a shear span-to-depth ratio of 0.27. The beams exhibited extremely brittle failure and produced average failure load of 199 kN and 281 kN for duplicate of specimens 1 and 2, respectively. The average shear failure loads for the equivalent longitudinally steel reinforced beams, duplicates of specimens 5 and 7, were 783and 937 KN, respectively. Nonetheless, the plain concrete beams' collapse mechanism was comparable to that of rein-forced concrete beams [14]. Shear failure of plain concrete is sudden since it undergoes a non-ductile behavior when experiencing tensile conditions [1, 15]. The purpose of the current experimental work is to examine the influence of changes in the shear span and loading arrangement on the shear performance of small-scale plain concrete deep beams. In such beams, shear transfer is governed exclusively by concrete tensile resistance, aggregate interlock, and compression zone action, without contribution from dowel action or

*Corresponding Author: anwzad@yahoo.com
Received 21 Jan 2026; Revised 04 Feb 2026; Accepted 04 Feb 2026
https://doi.org/10.36937/ben.2026.41109

transverse reinforcement. Moreover, the applicability of existing shear models to predict the shear capacity of plain concrete deep beams is investigated.

2. Experimental Methodology

The same concrete mix was used for casting the three groups of the specimens. Ordinary Portland cement, coarse aggregate with a maximum aggregate size of 19 mm, and river sand as a fine aggregate were used as ingredients for concrete with the same specific mix proportions of 1:1.9:2. All the specimens were rectangular in cross-section, 220 by 110 mm. The clear span for all the beams is shown in Table 1. All the beams were supported 50 mm from the two edges. For compressive and tensile strength, six cylinders with 100x200 mm were used for each group. All specimens and cylinders were cured under identical environmental conditions until the time of testing. For the three groups of beams, the shear behavior of specimens with one central point load (group A-1) and two concentrated loads (groups A-2 and A-3 beams) were investigated. For each group of 5 beams (e.g., A-1-1 to A-1-5 for group one), 5 values of shear span to overall depth ratio (a/h) were chosen to mainly examine the performance of small-scale beams under applied loads. All the beams were tested to failure using a 1000KN capacity universal testing machine, with the load incremented at a rate of0.5 kN and the final failure was load-controlled. The average compressive strength (fc) was 40.91, 41.8, and 42.14 MPa for the three groups. The same values of tensile splitting strength (fct) were 3.85, 3.71, and 3.97 MPa, respectively. The test results for the concrete, shear strength, and ultimate deflection are summarized in Table 1. Low value of std is observed for fc and fct test results.

Table 1. Experimental results for the tested beams

Specimen	Lcc* (mm)	fc (MPa)	fct (MPa)	a/h	P (KN)	Deflection (mm)	V (KN)
A-1-1	300	40.91	3.85	0.75	63.1	0.45	31.55
A-1-2	350	40.91	3.85	0.875	56.6	0.48	28.3
A-1-3	400	40.91	3.85	1.0	53.4	0.51	26.7
A-1-4	450	40.91	3.85	1.125	45	0.52	22.5
A-1-5	500	40.91	3.85	1.25	43.8	0.55	21.9
A-2-1	300	41.8	3.71	0.5	86.7	0.43	43.35
A-2-2	350	41.8	3.71	0.625	68.6	0.44	34.3
A-2-3	400	41.8	3.71	0.75	58	0.46	29
A-2-4	450	41.8	3.71	0.875	53.1	0.47	26.55
A-2-5	500	41.8	3.71	1.0	48.2	0.52	24.1
A-3-1	300	42.14	3.97	0.5	87.4	0.42	43.7
A-3-2	350	42.14	3.97	0.5	72.2	0.43	36.1
A-3-3	400	42.14	3.97	0.5	60.8	0.45	30.4
A-3-4	450	42.14	3.97	0.5	58.75	0.475	29.375
A-3-5	500	42.14	3.97	0.5	57	0.48	28.5
	Std	0.52	0.1				

* Lcc stands for the clear span of the beam.

3. Discussion of experimental results

3.1. Failure patterns

The load was applied gradually and the final failure load resulted in the rapid propagation of the crack. Fig. 1 shows the crack pattern for three identical deep beams of the same size with a clear span of 300 mm. The first specimen was tested under three-point loads, and it can be seen that the crack is under the point load, but it is not a clear vertical crack but rather an irregular vertical crack. When the duplicate of the same specimen was tested under four-point load with an a/h ratio of 0.5, the crack became more irregular compared with the one for the three-point loads. This trend continues when testing the triplicate of the beam for a lower a/h ratio of 0.375. The irregular crack originates from the bottom fiber of concrete beam, not in the middle distance between the two-point loads but rather near one of the point loads and propagates upward towards the compression concrete under the same load. The aggregate interlock mechanism is effective in transferring shear stresses across a small crack. Such transfer disappears with the increase in crack width. The crack patterns for three identical specimens with a clear span of 350 mm are depicted in Fig. 2. When the second similar specimen was tested under four-point loads with an a/h ratio equal to 0.625, the crack became more inclined compared to the first similar specimen tested under three-point loads. When the third similar specimen was tested for an a/h ratio of 0.5, the crack initiated at the center of the bottom fiber and gradually became irregular and curved in shape. The failure mode was affected by the a/h ratio to a large extent, and no beam failed in flexure or right at mid-span, where a main vertical crack is expected. Therefore, no specimen experienced any direct flexural distress.

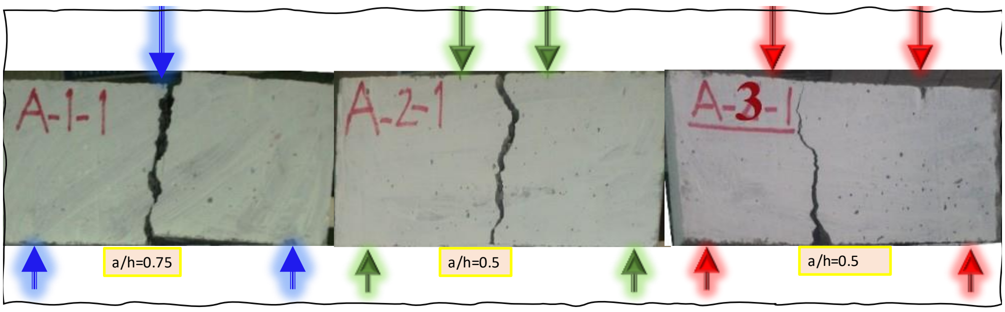

Figure 1. Effect of a/h ratio on the cracking pattern of beam A-1

Deep beams lack post-peak ductility due to sudden, brittle rupture. The failure pattern for beams with a clear span of 400 mm is illustrated in Fig. 3. The shear strength of DB is affected by the aggregate interlock mechanism in the cracked tensile concrete and shear force in the concrete compression zone at early stages of loading. However, with the increment in the load, the first mechanism diminishes with the opening in the crack width. The same thing is correct for the second mechanism. One exception in the crack pattern can be seen for the beam A-1-3, with three-point loads. There are two small cracks at the lower bottom center of the beam. These two cracks joined together with the increment in the load and continued moving upward in the direction of the applied load. The similar beam (A-2-3) when subjected to four-point loads had the crack shifted close to the one of the loads instead of being in the center of the two loads. The crack shape for the third similar specimen (A-3-3) became more irregular when the a/h ratio was 0.625. The formed macro-crack changed the original shape of the specimen, by splitting it into two parts, and restricted the deformability of the concrete. The crack angle varied between 40 and 60^{o} for tested beams. The maximum coarse aggregate size affects the Aggregate Interlock mechanism. For the tested beams a maximum aggregate size of 19 mm was used in a relatively small 110 mm wide beam. The ratio of aggregate size to beam width was relativly high leading possibly to significant improvement in the roughness and sliding resistance.

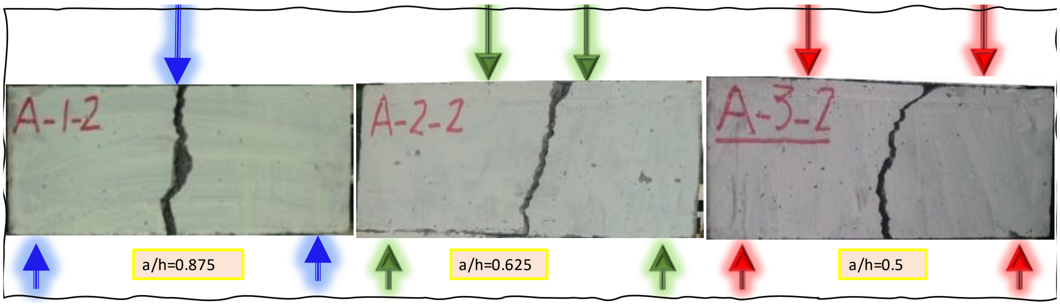

Figure 2. Effect of a/h ratio on the cracking pattern of beam A-2

Plain concrete cannot tolerate deformation cracks, which have a detrimental effect on its structural integrity. In the absence of tensile softening, Shear collapse in such members is controlled by tensile cracking and fracture propagation, which is related to fracture mechanics concepts. Fig. 4 demonstrates triplicate beams with a clear span of 450 mm. As can be seen, the crack is semi-vertical for the case of one-point load beam. Whereas, when the similar beam was tested under four-point loads, the crack became more irregular and shifted close to one of the point loads. This irregularity and crack inclination continued when the third similar beam was tested for an a/h ratio of 0.75. The failure pattern of the three identical beams with a clear span of 500 mm is presented in Fig. 5. When tested under three-point loads, the crack was under the load but not completely vertical. However, when tested under two-point loads, the crack was slightly inclined towards one of the point loads. Moreover, when its identical beam was tested for an a/h ratio of 0.875 under four-point loads, the crack became more inclined in the upper half of the beam. It can be said that generally for the beams tested under three-point loads the crack was nearly vertical but irregular in shape.

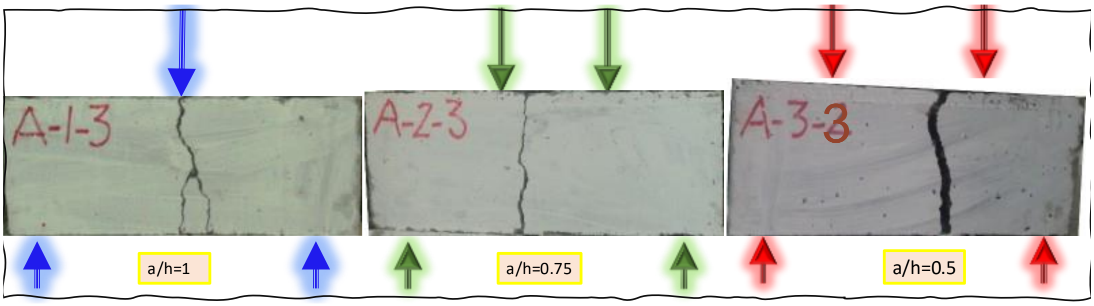

Figure 3. Effect of a/h ratio on the cracking pattern of beam A-3

On the other hand, when the specimens were tested under four-point loads, the single crack became inclined or tilted to one side of one of the loads in the upper half of the beam. All fracture surfaces exhibited significant macro-roughness, i.e., the failure of the plain concrete DB was not similar to the failure of a notched beam where the crack is pre-controlled and more regular in shape. Generally, deformation and ductile behavior are not essential features of the design of plain concrete beams. The testing modifies the failure mechanism of the plain concrete DB and is not merely a pure shear. The modes of failure of plain concrete deep beams are different from flexurally distressed specimens, in the absence of steel reinforcement. The presence of steel reinforcement hinders the opening and growth of cracks, allowing more concrete deformations and ductile behavior. Moreover, the bond between concrete and steel bars contributes to the strength of beam specimens.

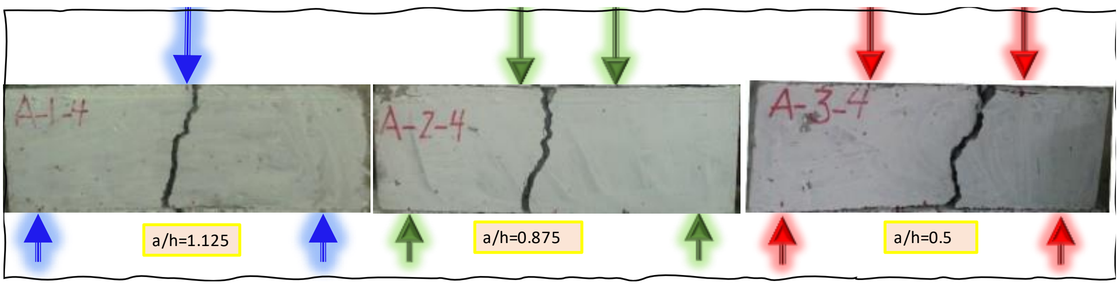

Figure 4. Effect of a/h ratio on the cracking pattern of beam A-4

Although the specimens were tested for shear, deviation of the failure from the anticipated shear failure was observed. Even more important is the sliding of concrete along a plane parallel to the applied loads' direction was not achievable since the applied load exceeded the shear capacity of concrete. The nonlinear deformations result only in a single macro crack crossing the beam until the complete separation. All the energy was dissipated through the macro crack propagation. The stability throughout the test is difficult to achieve in plain DB, and the crack location was not controlled [16].

3.2. Load-deflection

The load-midspan deflection relationship for all the plain concrete deep beams is depicted in Figs. 6 to 8, respectively. As can be seen, there is nearly a linear relationship at the start. This linear relationship remained largely unchanged even at higher load levels. As the clear span or the a/h ratio was increased for the three-point loaded DB, the deformation capacity was increased. The maximum achievable change in deformation was 22% for the beam A-1-5 compared with beam A-1-1. For groups two and three beams, A-2 and A-3, the load-midspan deflection relationship was relatively more linear (Figs. 7 and 8). This was due to the more brittle failure experienced by the two groups.

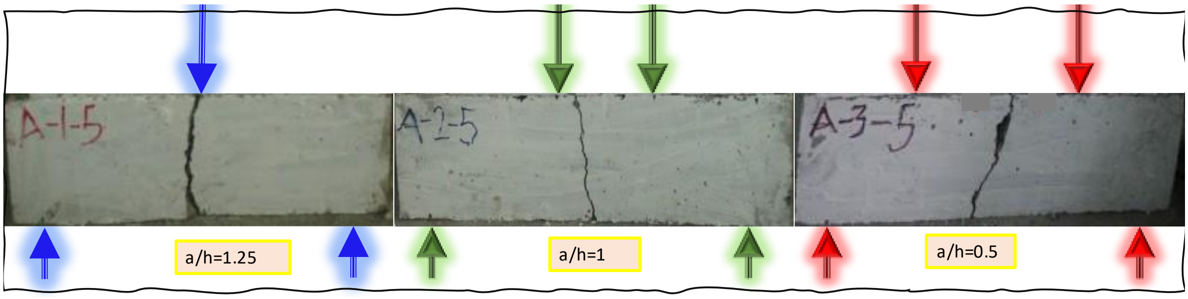

Figure 5. Effect of a/h ratio on the cracking pattern of beam A-5

The change in deflection was associated with the loading level experienced by each beam. Overall, the deformation capacity incremented with an increase in a/h, except for beam A-3-1, which exhibited exceptional deformations.

3.3. Shear behavior

The shear strength of beams is adversely affected by the increase in the shear span-to-overall depth ratio. In section 3.1, the failure mode of plain concrete beams was shown to be sensitive to the a/h ratio. Therefore, the shear failure of beams with constant depth is plotted against shear span/overall depth in Fig. 9. Specimens A-2-1 and A-3-1, Figs. 9(b) and 9(c), exhibited failure loads that were 37.4% and 38.5% greater than that of specimen A-1-1, Fig. 9(a).

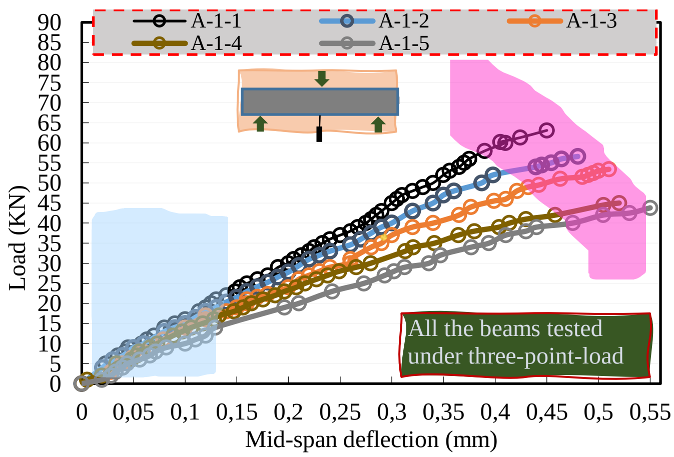

Figure 6. Load versus mid-span deflection for the beams of group A-1

The variability in experimental shear value increased with a decrease in the a/h ratio, resulting in the reduction in the Pearson's correlation coefficient. Hence, the slope of the linear trending line increased with the change in loading from three-point, Fig. 9(a), to four-point loads, Figs. 9(b) and (c). Moreover, the correlation between the shear load and the a/h ratio was sensitive to the load configuration.

3.4. Shear span-overall depth ratio

Due to the change in the a/h ratio, the slope of the best-fitting line changed with the altering in the load configuration. This line is less steep for the plain concrete DB of group A-1, Fig. 9(a), compared with its equivalent beams tested in groups A-2 and A-3, Figs. 9(b) and (c). The deformation capacity was also affected by the change in the a/h ratio. The maximum deflection of deep beams A-2-5 and A-3-5, Figs. 10 (b) and (c), were 5.5% and 12.7% lower than that of beam A-1-5, Fig. 10 (a). Although all the beams did not establish the same level of shear strength, this parameter was confirmed to be a critical parameter for the design of plain concrete DB's. This shows that direct consideration of the shear span-to-overall depth ratio is an efficient technique for evaluating the performance of plain concrete DB's.

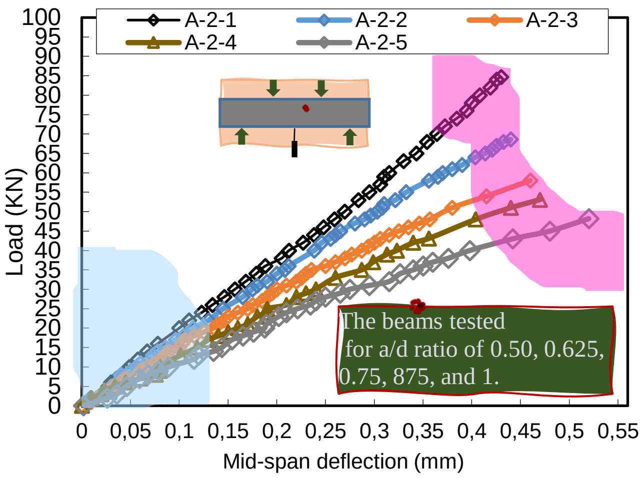

Figure 7. Load versus mid-span deflection for the beams of group A-2

4. Shear models and critical parameters

In plain concrete beams, shear resistance is governed primarily by tensile cracking, aggregate interlock, and compression zone action, without any stabilizing contribution from reinforcement. These mechanisms differ not only quantitatively but also qualitatively from those in reinforced members. Thus, two crtical parameters, compressive strength and a/h ratio, influence the shear performance of plain concrete DB in the absence of main longitudinal and secondary shear reinforcements. Hence, shear in plain concrete deep beams is a fracture-dominated phenomenon rather than a redistribution-based mechanism. A non-linear relationship between shear strength of concrete and compressive strength was reported [17]. Furthermore, the shear strength of concrete is usually taken into account by most of the standard codes. This is important in order to achieve the best possible design.

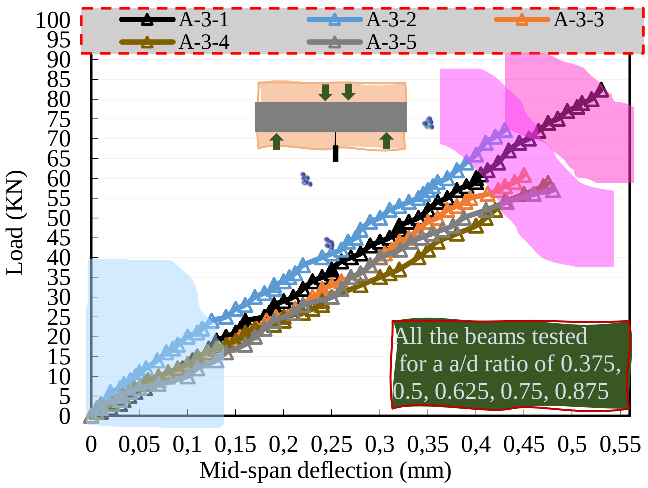

Figure 8. Load versus mid-span deflection for the beams of group A-3

4.1. Evaluation Metrics

The prediction consistency of the current relevant shear models in estimating the ultimate shear strength of plain concrete DBs was evaluated using four assessment metrics. These included the minimum/maximum ratio (min/max), average, standard deviations (std), and covariance (cov) of predicted/experimental shear. In addition to the absolute average error (AAE) between the predicted and experimental shear values.

4.2. Existing shear models

The compressive strength is the key parameter that most of the existing shear models are built on. This is either as a single parameter like in ACI code 318-14 equation [7] or in combination with other parameters [24].

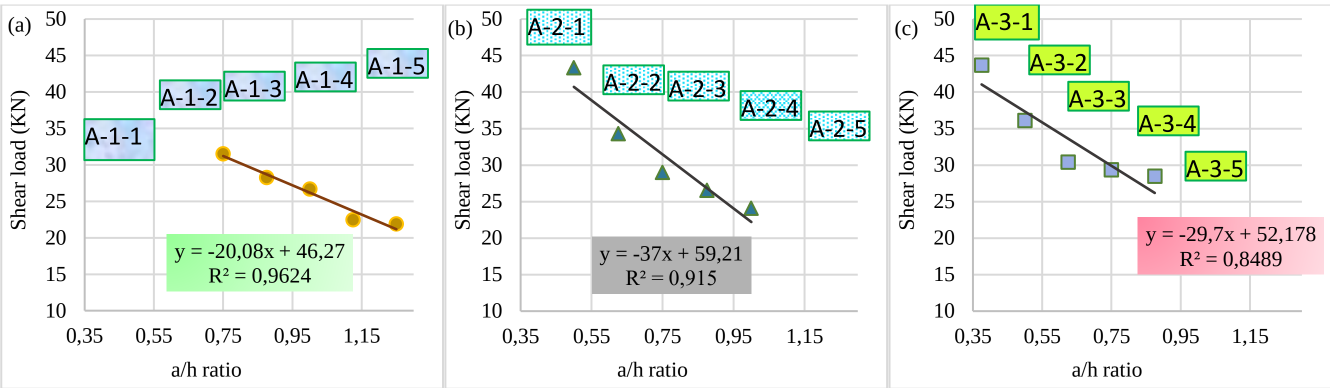

Figure 9. Load versus a/d ratio for beam groups of: (a) A-1, (b) A-2; (c) A-3

Only a few equations are based on the tensile splitting strength of concrete and exclude the compressive strength of concrete, e.g., GB50010-2010 [39], BEAL French code [29], Chinese Standard YB 9082-2006 [32], Norwegian Standard NS 3473 [26], and Desai [33]. The second key parameter is the main longitudinal steel ratio, which has been incorporated into these models [31, 22, 24]. The third key parameter is the span-effective-depth ratio (a/d ratio), also known as M/Vd, which has been adopted by a number of shear models [19, 39, 44, 46]. However, some of the shear equations are also based on additional or other parameters, such as the coarse aggregate size [24], steel yield strength [49], secondary steel [49], and recycled coarse aggregate ratio [44].

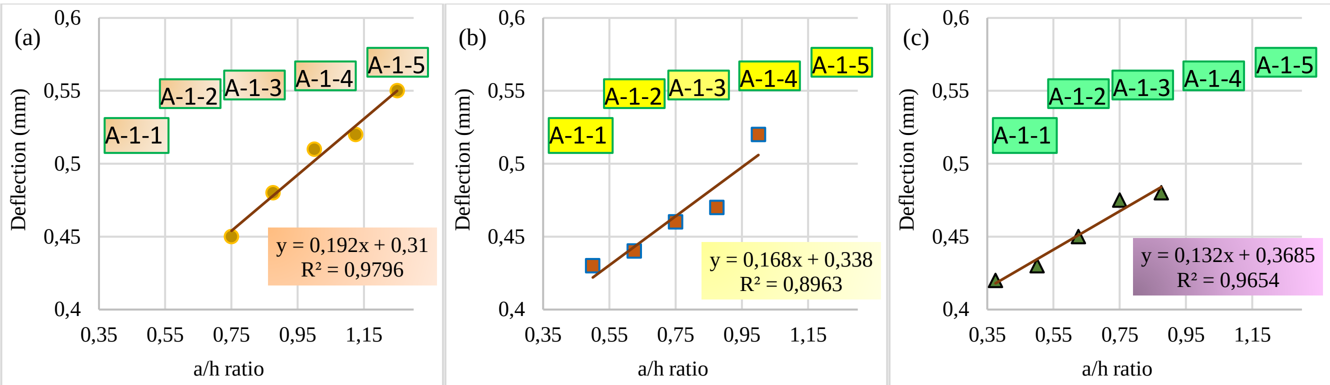

Figure 10. Deflection versus beam number for beam groups of: (a) A-1; (b) A-2; (c) A-3

4.3. Applicability of shear models

To determine the shear capacity of short-span DB without both longitudinal and transverse reinforcement, the predictions from existing design techniques and models were evaluated. Only models that would not cancel out because of the lack of specific criteria, like primary longitudinal steel or secondary shear steel, were taken into consideration. In these models, the aforementioned two parameters were replaced with zero instead of being cancelled out. Moreover, other existing shear models, which will result in zero values of shear strength due to their formulation, were eliminated from the analysis. Therefore, from existing shear equations, only thirty-five models ACI318–19; Moretto, 1945; Clark, 1951; Bresler and Scordelis, 1963; Rajagopalan and Ferguson, 1968; ASCE-ACI Committee 426, 1973; Walraven and Reinhardt, 1981; NZS, 1984; Mphonde et al., 1984; NS 3473, 1989; AASHTO, 1994; Collins and Kuchma, 1999; BAEL., 199; Khuntia et al., 1999; TS500, 2000; JGJ 138-2001, 2002; Desai, 2004; YB 9082-2006, 2007; ISIS, 2007; Arslan, 2008; KBC, 2009; AISC 360-10, 2010; GB50010-2010, 2011; CEB-FIP, 2012; NBR 6118, 2014; ECP 203–2017, 2017; Rahal and Alrefaei 201; Etman et al., 2018; CSA-A23.3- 19, 2019; Okamura and Higai, 1980; Mansur et al., 1986; Hedman and Losberg, 1978; Mphonde and Frantz, 1985) from thirty-five references [7, 18-49] were applicable for the analysis. The findings of the comparisons between the observed shear strengths of plain concrete deep beams and the predictions from the applicable shear models are graphically displayed in Figs. 11 to 13. Three types of relationship are observed between the predicted shear from the 35 equations and the experimental shear results, as explained in the following sections.

4.3.1. Uni-linear relationship

There is a unilinear relationship between the predicted and the 15 experimental shear values. The predicted shear values and their equivalent experimental values fall on a single linear trendline that passes over all fifteen data points. Fig. 11 shows the first type of relationship. These models produce the same or similar shear values for the predicted strength of fifteen tested beams. The pattern of relationship is similar for all the models in this group. The Pearson's correlation coefficient (R^2) is very small and it is the same for all these models. It is equal to 0.24 and the R value is equal to zero. The main reason for this is that these models ignore the arch effect or role of the a/h parameter.

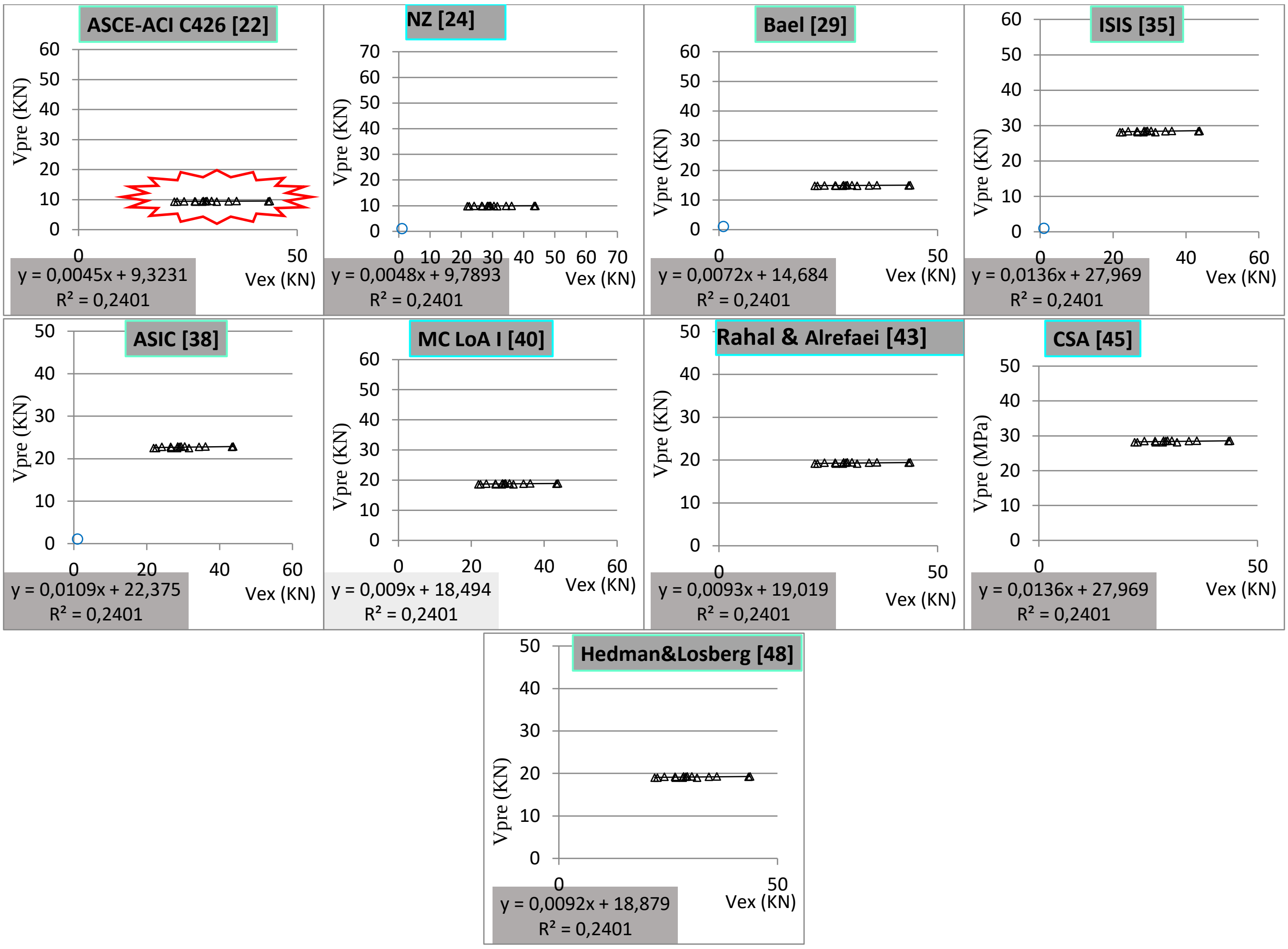

Figure 11. Predicted shear using models [22, 24, 29, 35, 38, 40, 43, 45, 48] versus experimental shear

All models in this group produce conservative estimations of the shear capacity, for example, models [22, 24, 29, 40] and [48]. The other models in Fig. 11 are less conservative. However, the difference among the predicted shear values for the three groups of beams (A-1, A-2, A-3) is either small, there is no difference like model [20], or there is a very small difference in fractions of decimals like model [45].

4.3.2. Tri-linear relationship

Similar predicted shear values for each of the five beams or each group of tested beams are yielded by the related shear models. Therefore, in reality, the relationship between the predicted and experimental data is expressed by three lines, Fig. 12. For each group, there is a single predicted shear value. The predicted-experimental data points for each group of beams are highlighted with a red circle in Fig. 12 for the ACI code 318-14 [7], where the upper set of five data points are for group A-3 with the highest compressive strength. The next sets of data are for groups A-2 and A-1, respectively. This is because these models depend on the compressive strength of concrete as a single critical parameter, for example, the ACI code 318-14 [7], or the compressive strength of concrete is the main parameter among other parameters. The linear trendline passes through one point of test results for groups A-3 and A-2. The other data points are left out away from the trendline, including group A-1 data points. Bearing in mind that a trendline might not pass through all points in a graph, which is acceptable. However, returning a single shear value for a group of five different beams (A-3) by a model is a point of weakness and needs further research and improvement of its generality. The correlation between the predicted and experimental shear is poor, and the R^2 value is either small and equal to 0.24 [7] or very small and equal to 0.0137 [33]. The R value= 0.22. Overall, the difference among the predicted shear values for the 15 beams is small for all the models. However, some predictions are conservative, such as model [28], while others are unconservative like models [18, 21].

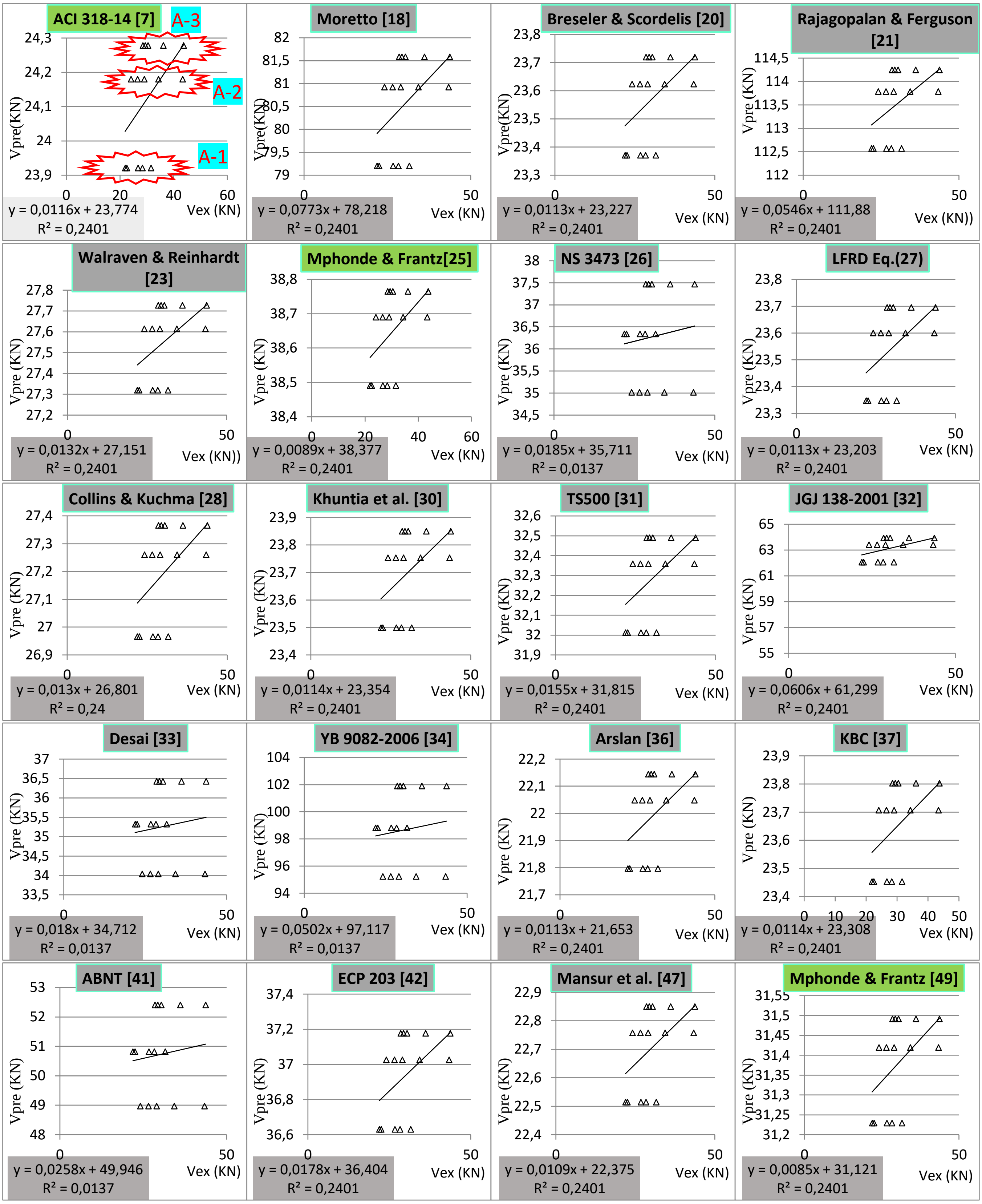

Figure 12. Predicted shear using models [7,18,20,21,23,25,26,27,28,30,31,32,33,34, 36,37,41,42,47, 49] versus experimental shear

4.3.3. Bi-linear relationship

The third type of relationship is shown in Fig. 13. Actually, the relationship between the predicted and

experimental data is expressed by two lines. One line is the linear trendline, which passes through or near most or some of the data points. The other line, which is an imaginary line representing group A-3. Therefore, this group of beams are highlighted with a red circle in Fig. 13. That is because one single shear value is predicted for the five different beams tested for a constant a/h ratio. Overall, there is a better prediction for groups A-1 and A-2. This is because these models encounter the influence of the shear span/overall depth ratio in their formulation. Unlike some other models, the a/h ratio in four models grouped in this section [19, 39, 44, 46] is independent or not multiplied by the main steel ratio. The four models yield higher values of the correlation coefficient, with values between 0.5 and 0.58. The R value= 0.085. However, one shortcoming of these models is when predicting the shear capacity of group, A-3 beams with a constant a/h ratio of 0.5, they yield a single shear value for the five different beams in group A-3. Three models [19, 39, 46] overestimate the test results, while one model [44] underestimates them.

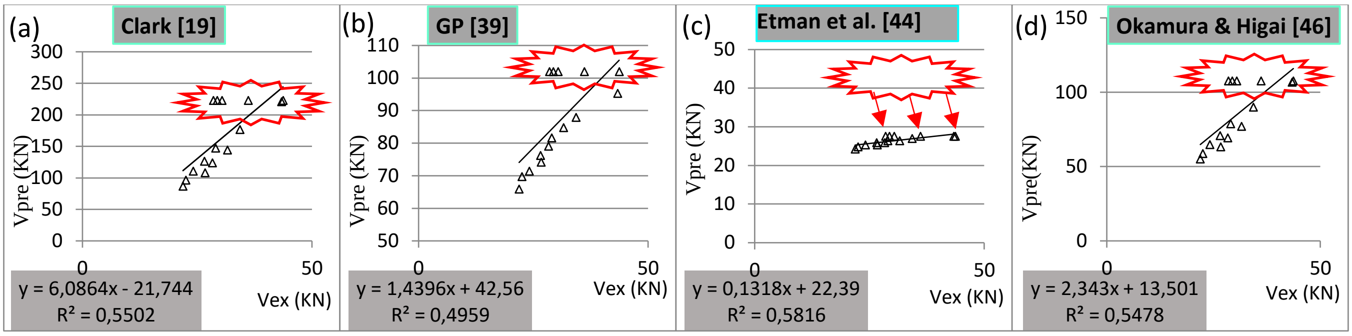

Figure 13. Predicted shear using models [19, 39, 44, 46] versus experimental shear

4.4. Shear model performance

In order to compare the shear models and make a direct comparison among the model performance for each group of beams, the predicted-experimental shear is plotted in Figs. 14 to 16 for the three groups of plain concrete deep beams. As mentioned earlier, the steel ratio was not eliminated when predicting the shear strength of plain concrete beams; instead, it was replaced with zero. This is true for other parameters that they use to formulate these models.

4.4.1. Group one beams, A-1

As shown in Fig.14(a), the navy-blue color line indicates the experimental results. The Clark equation [19] is one example of a model that significantly overestimates the shear capacity of plain concrete beams. Other predictions were close to experimental values, as depicted on the opposite right-hand side of Fig. 14.

(a). As can be seen, for group number one, most of the shear models overestimate the shear capacity of beams A-1-4 and A-1-5. In contrast, most of the models underestimate the shear capacity of beam A-1-1. The five statistical matrixes for group number one are shown in Fig. 14(b). The red line, which intercepts the Y-axis at two, represents perfect correlation between experimental and predicted values for each one of the thirty-five models. As seen, this value of two is calculated from the summation of five indexes: min/max, average, and std, cov, and AAE. A perfect match between the experimental and evaluated shear levels is represented by the value of two, min/max=1, and average=1. The remaining indexes' summation equals zero. With the exception of models [20, 29, 36, 37, 43], which exhibit reasonable prediction and fall within the limit of two, the majority of these values are either above or below the red line.

4.4.2. Group two beams, A-2

The change in a/h ratio for group two has little effect on the Models' prediction, as shown in Fig. 15(a). The majority of models have a linear prediction, meaning that as a/h ratio changes, the model prediction remains unchanged. Nonetheless, a few model predictions result in a non-linear correlation with the experimental results. These models are [19], the highest red-dashed curve, followed by the two curves for models [39] and [46]. When compared with group one beams, a similar trend is observed for group two beams regarding the five indexes. The summations of five indexes are either above or below the red line. There are no models with perfect predictions.

4.4.3. Group three beams, A-3

The predicted-experimental shear for group three, A-3, is depicted in Fig.16. It is evident that almost all models failed to capture the experimental behavior of group A-3 and reflect the effect of keeping a/h constant on the predicted shear values. Only the shear capacity of beam A-3-5 can be evaluated reasonably. The adjustment in the a/h ratio has little effect on the majority of the model's predictions.

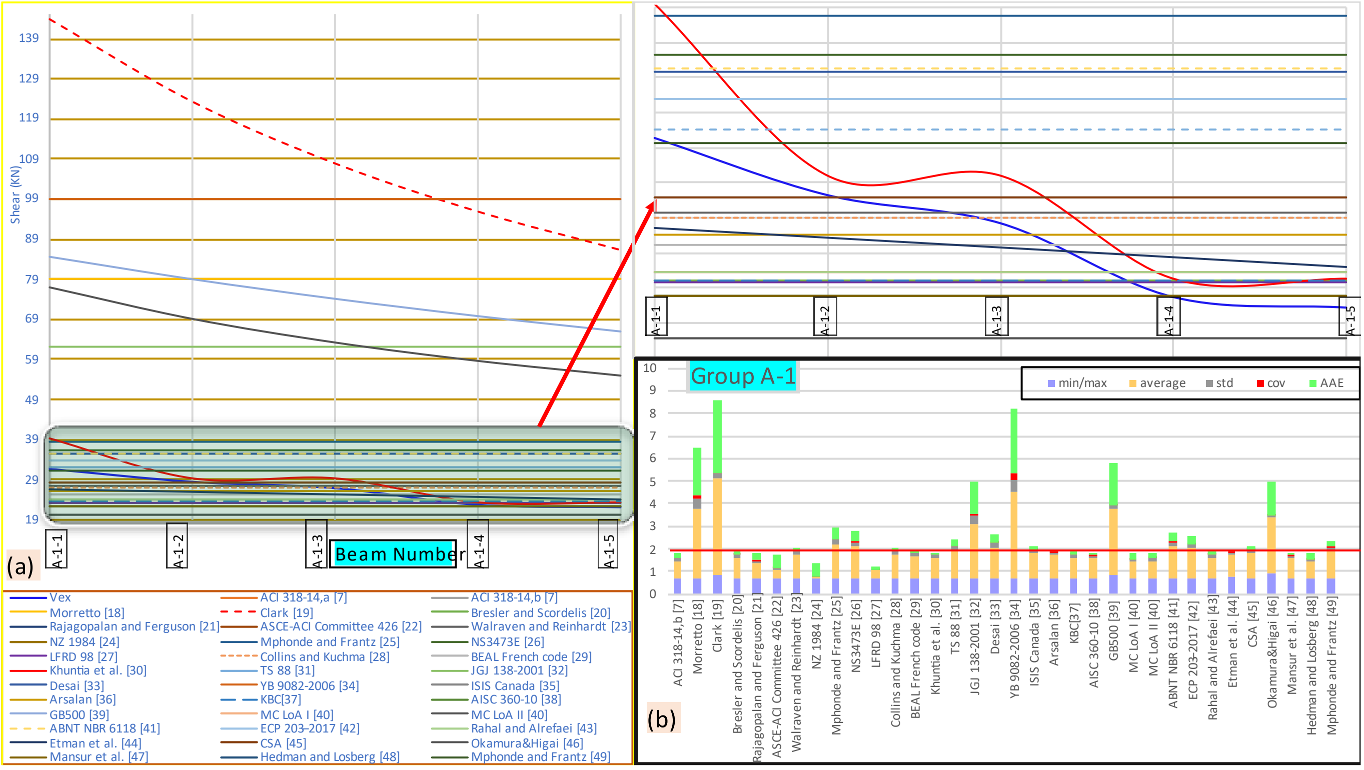

Figure 14. Predicted shear and statistical metrics for group one beams (A-1)

Although the Arsalan's model [36] shows some deviations from linearity. Once more it is evident that there are models that significantly overestimate the shear capacity like Clark's model [20]. While others underestimate. The error between the experimental and projected shear values is reduced by models [21] and [22], Fig. 16 (b), but not eliminated. For some models, this error spikes up multiple times.

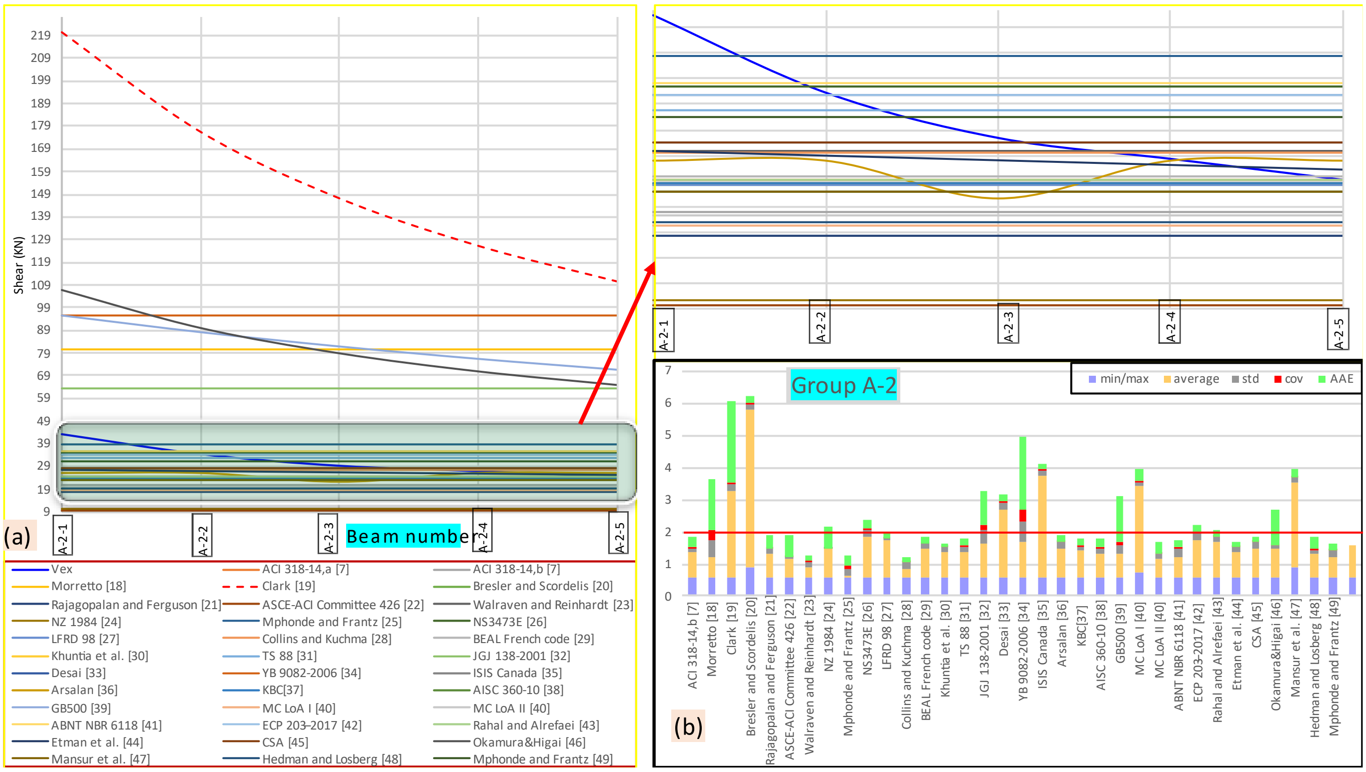

Figure 15. Predicted shear and statistical metrics for group two beams (A-2)

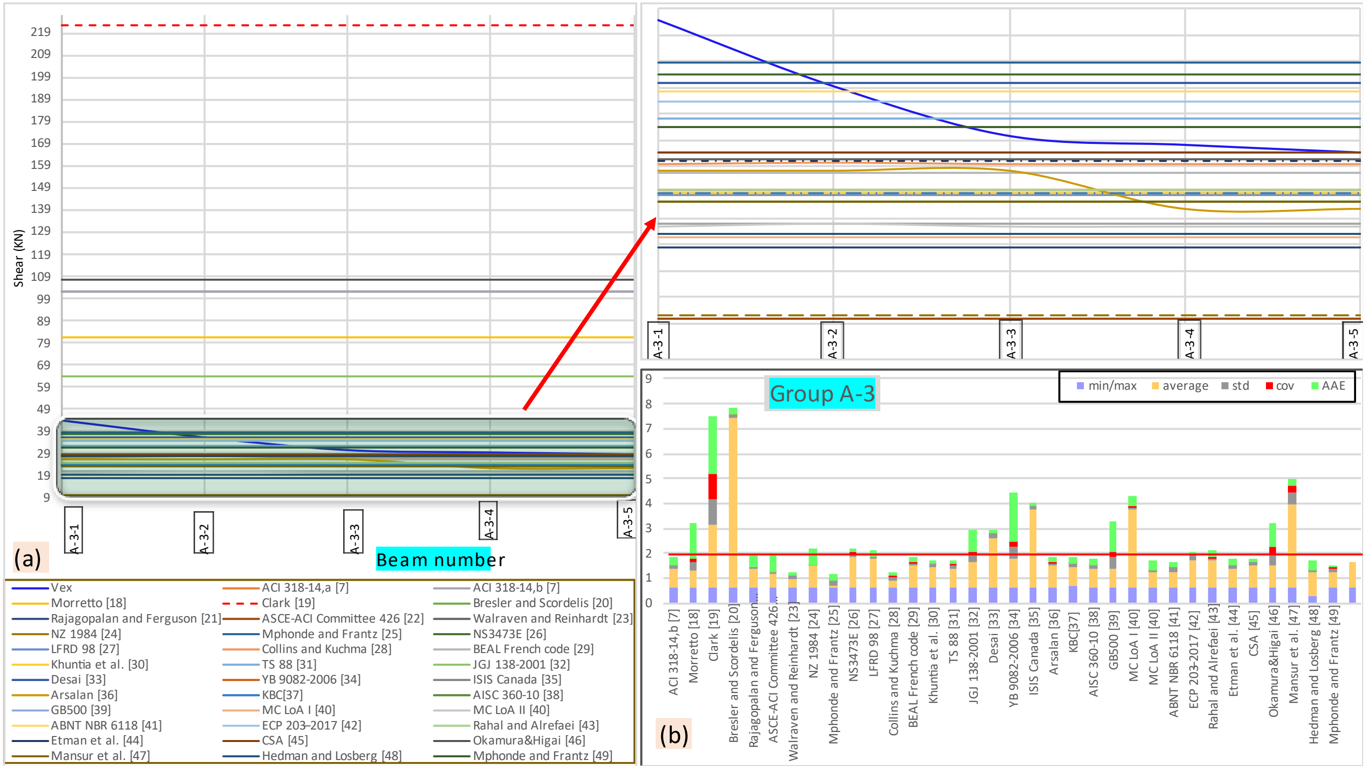

Figure 16. Predicted shear and statistical metrics for group three beams (A-3)

4.5. Shear model for plain concrete DB

Plain concrete is weaker in tension than in compression. Under the load, the bottom fiber of a plain concrete deep beam typically ruptures under tension, leading to failure. This type of failure is presumed since it is expected that the concrete at the location of the highest stress will break and fracture. Therefore, this element represents a crack-controlled tensile stress field. Moreover, the compressive strength of concrete is higher than its tensile splitting strength; thus, the rupture of the supporting tension element at the bottom fiber, which achieves the highest stress under tension, is anticipated to cause failure in a plain concrete deep beam. This condition occurs when the tensile stress within the fracture-controlled tension tie equals the concrete tensile strength (fct).

So far, no research has examined the shear behavior of plain concrete deep beams. Nonetheless, one study suggested the possible use of the strut-and-tie model for plain concrete deep beams [50]. In the present work, an attempt is made to simulate the failure of plain concrete deep beams using a simple strut and tie model (STM). Therefore, it is expected that one type of strut is formed in a plain concrete deep beam, and that is the compression strut. However, the struts need a tie. Hence, a concrete tie is assumed here in order to replace the lost tie, longitudinal flexural reinforcement. The struts and the tie are denoted by solid lines, as shown in Fig. 17. The STM for a three-point load is depicted in Fig. 17(a), whereas the four-point load is depicted in Fig. 17(b). Nonetheless, the size of the equivalent tensile stress path is important. For that, figuring out the k_t value is essential. An attempt is made to find the k_t values for the small-size plain concrete deep beams that were tested in this present investigation. Using the lever arm of h and the basic bending hypothesis, k_t was taken as 0.167. However, Kumar [50] assumed a value of 0.15 for the k_t. Using regression analysis, in the current study the value of k_t was found to be 0.14. Consequently, the failure load was assessed using:

$$V_{th} = \frac{2}{\frac{a}{h}} f_{ct}(k_t bh) \tag{1}$$

Where $k_t bh$ is the size of the equivalent tensile stress path assumed to be in tension.

4.5.1. Modifications to fix linearity

The shear span-overall depth ratio was kept constant for all the five DB's tested in group three. As explained earlier, for each shear model all the predicted shear values were equal. That meant one single prediction for the five beams in group three instead of five different predictions. All the thirty-five models failed to reflect the effect of keeping a/h constant on the predicted shear values of group three, Fig. 16. This is despite the differences in the supported-span between the five specimens in group three. To resolve this issue, Eq. (1) was modified in order to avoid the predicted shear data points falling on horizontal line when plotted versus the experimental shear values.

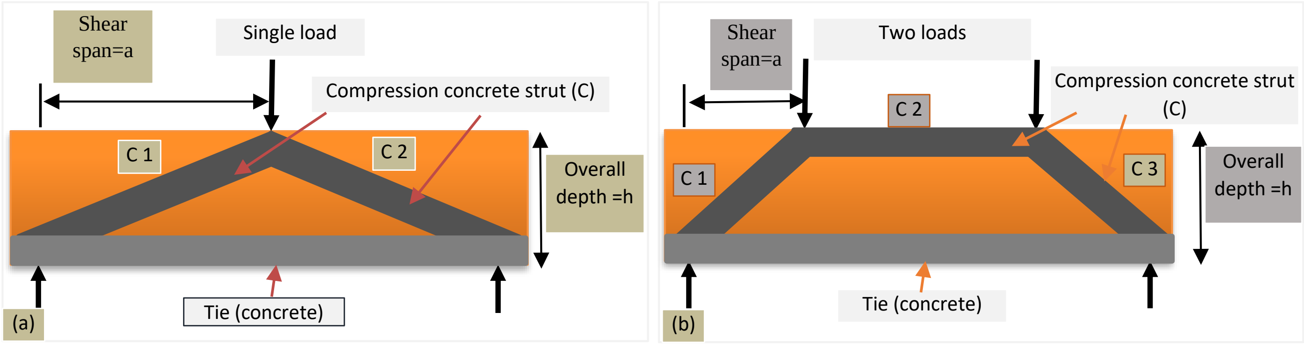

Figure 17. Compression and tension struts in a plain concrete deep beam subjected to: (a) three-point-load; (b) four-point-load.

Hence the failure load was evaluated from:

$$V_{th} = \frac{2}{\frac{a}{h}} f_{ct}(0.14bh) * \left(\frac{L-L_{cc}}{L_{cc}}\right)^{0.12} \tag{2}$$

Where, L equal to the overall length and L_{cc} represent the span of deep beam. The power constant (0.12) is an empirical adjustment factor and applicable to current test data. The predicted shear capacities: for the groups one and two, using the proposed model Eq. (1), and for group three using Eq. (2) were plotted against the experimental results in Fig. 18. The correlation coefficients are extremely strong, as is seen for groups one and two, where R^2 equals to 0.99 and 0.96, respectively. As can be observed, group one's index submission is slightly above two, which is the ideal prediction. Group two's index summation is also slightly above two, with the sum of the five indices equal to 2.25. Because the span overall depth is constant for the beams evaluated in group 3, equivalent shear predictions are made with a similar a/h ratio since the shear span is also constant. As a result, the accuracy of predictions for group 3 is high using Eq. (2), and R^2 equals 0.9.

Fig. 18 shows that for group three beams, the horizontal linear buildup of five equal predicted shear data points associated with the thirty-five models is largely eliminated and replaced with five different predicted shear data points. The summation of five indexes for the group three is equal to 3.17. However, the average AAE value for the three groups of tested deep beams is 12.9%. The same value for the shear models [20, 29, 36, 37, 43] is 22%, 18%, 17%, 21%, and 20%, respectively.

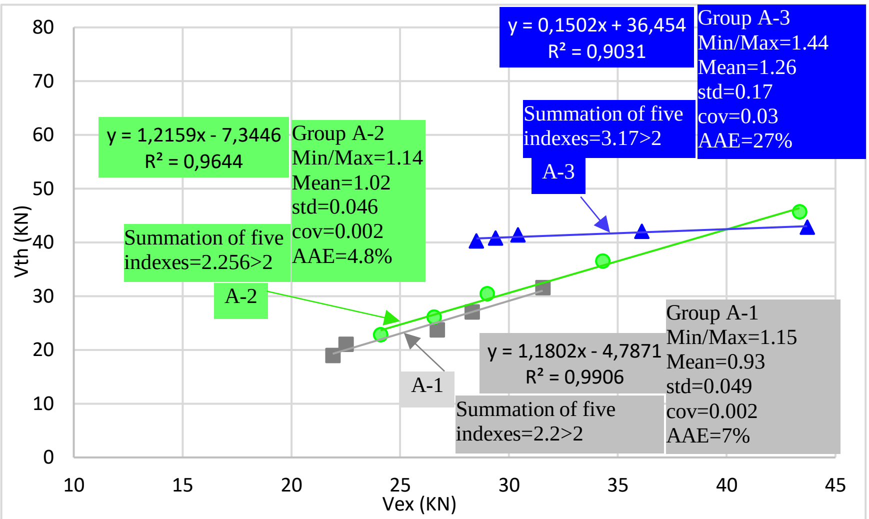

Figure 18. Predicted versus the experimental shear for the three groups of plain concrete DB's using the proposed simplified and modified STM

4.6. limitations of the proposed shear model for plain concrete DB

More investigations are needed to highlight the constraints related to the limited experimental scope, the lack of external validation, and the scale and size effect. Research is needed to examine and verify the applicability of the proposed model for larger beams since the absolute shear values may not be scaled linearly. With larger dimensions of beams the size effect becomes a critical parameter resulting in predictions above the experimental values [51]. Another limitation of the present study is relating crack inclination to shear-span ratio or interpreting crack localization through simplified strut inclination, which will further improve the proposed simplified STM.

4.7. Recommendations and future directions

Structural plain concrete can be designed based on the tensile strength of concrete. Since it is brittle, restraint from creep, temperature, and shrinkage can result in tensile stresses leading to uncontrolled cracks. Several decades ago, design codes for the structural performance of reinforced concrete were developed. Continuous research and new construction materials will make the design codes continue to evolve, and this will make practicing engineers alter their way of design [17].

5. Conclusions

This study investigated the shear capacity of plain concrete deep beams by testing fifteen beams. In light of the experimental results, the following conclusions can be drawn:

- Shear failure of plain concrete deep beams is characterized by a sudden and brittle failure. The two groups, A-1 and A-2, experienced more brittle failure than group A-1. The crack was almost vertical for the beams tested under three-point loads. However, the single crack shifted close to one side of one of the loads when the specimens were tested under four loads. All the crack surfaces were rough and irregular in shape.
- The relationship between load and midspan deflection was comparatively more linear for groups two and three beams, A-2 and A-3, compared with group A-1.
- 3- As the a/h ratio decreased, the experimental shear's variability increased.
- In the absences of both flexural and shear reinforcements, only thirty-five models among the existing shear equations for normal reinforced concrete beams were applicable to predict the shear capacity of plain concrete deep beams. The majority of the applicable shear models are conservative. Nevertheless, the remaining models produced predictions that were unsafe.
- All the applicable shear models failed to capture the experimental behavior of group A-3 and reflect the effect of keeping a/h constant on the predicted shear values. Each model prediction was similar for the five different plain concrete deep beams in group three.
- A strut-and-tie model for the shear capacity of small-sized plain concrete deep beams is proposed. The proposed model yielded better shear predictions compared with all the thirty-five current shear models that were applicable to the specimens tested in the present investigation. The proposed model was modified for group three to account for the effect of the constant a/h ratio but, with different clear spans. The summation of five indexes for group three is equal to 3.17. However, the average AAE value for the three groups of tested deep beams is 12.9%. The same value for the predicted shear using the five best performing model among the thirty-five is [20, 29, 36, 37, 43] is 22%, 18%, 17%, 21%, and 20%, respectively.

Two important factors affecting the structural of plain concrete DBs are the shear span/overall depth ratio and the type of applied load and. A comprehensive examination of the current formulas for calculate-ing the shear strength of plain concrete deep beams was conducted. More testing is required for future studies in order to study the shear strength of plain concrete deep beams with crushed coarse aggregate and with steel fibers. Additionally, the effect of cementitious ingredients and byproducts on the ability of concrete to withstand shear loads is critical. This will help to gain a better understanding of the function and contribution of concrete in reinforced concrete beams. It is expected that the current study will pave the way and open up new paths for research and innovation in this area.

Declaration of Conflict of Interests

The author declares that there is no conflict of interest. They have no known competing financial interests or personal relationships that could have appeared to influence the work reported in this paper.

References

[1.] Majdzadeh, F., Soleimani, S.M. Banthia, N. Shear strength of reinforced concrete beams with a fiber concrete matrix. Canadian Journal of Civil Engineering 33 (2006), 726-734.

[2.] Clark, A. P. Diagonal Tension in Reinforced Concrete Beams. Journal of the American Concrete Institute 23 (1951)145-156.

[3.] Smith, K. N., Vantsiotis, A. S. Shear strength of deep beams. ACI Journal 79-3 (1982) 201-213.

[4.] Sagaseta, J., Vollum, R. Shear design of short-span beams. Magazine of Concrete Research 62 (2010) 267-282.

[5.] Lu, W. Y., Lin, J., Yu, H.W. Shear strength of reinforced concrete deep beams. ACI Structural Journal 110(2013)671.

[6.] Muendacha, D., Teerawong, J. Chetchotisak, P. A safety-based evaluation of strut-and-tie methods for shear design of RC deep beams in accordance with international concrete codes. Engineering and Applied Science Research 47(2020)137-144.

[7.] ACI318–14. Building Code Requirements for Structural Concrete; American Concrete Institute: Farmington Hills, MI, USA, (2014).

[8.] Giaccio, G., Tobes, J.M. and Zerbino, R. Use of small beams to obtain design parameters of fibre reinforced concrete. Cement and Concrete Composites 30(2008) 297-306.

[9.] Shajil, N., Srinivasan, S.M., Santhanam, M. Self-centering of shape memory alloy fiber reinforced cement mortar members subjected to strong cyclic loading. Materials and structures 46(2013) 651-661.

[10.] Khaled M., Özgür E., Hooman, R. The Influence of Amount and Aspect Ratio of Fibers on Shear Behaviour of Steel Fiber Reinforced Concrete. KSCE Journal of Civil Engineering 21 (2017) 1393-1399. DOI 10.1007/s12205-016-0787-2- 1393 -pISSN 1226-7988, eISSN 1976-3808.

[11.] Al-Ta'an, S.A., Al-Feel, J.R. Evaluation of shear strength of fibre-reinforced concrete beams. Cement and Concrete Composites, 12 (1990)87-94.

[12.] Paulay, T. and Loeber, P.J. Shear Transfer by Aggregate Interlock, Shear in reinforced Concrete, ACI Special Publication 42(1974) 1-15.

[13.] Minelli, F. Plain and fiber reinforced concrete beams under shear loading: Structural behavior and design aspects (2005) 1-428.

[14.] Campione, G., Minafò, G. Behaviour of concrete deep beams with openings and low shear span-to-depth ratio. Engineering Structures, 41(2012) 294-306.

[15.] Moghadam, M.A., Izadifard, R. Evaluation of shear strength of plain and steel fibrous concrete at high temperatures. Construction and Building Materials, 215(2019) 207-216.

[16.] Barr B., Gettu, R., Al-Oraimi S. K. A., Bryars, L.S. Toughness measurement – the need to think again. Cem Concr Compos 18(1996)281–97.

[17.] Tabsh, S.W., Safety of reinforced concrete members designed following ACI 318 building code. Engineering Structures 19(1997) 843-850.

[18.] Moretto, O. An investigation of the strength of welded stirrups in reinforced concrete beams. In Journal Proceedings 42(1945) 141-164.

[19.] Clark, A.P. Diagonal tension in reinforced concrete beams. In Journal Proceedings 48(1951) 145-156.

[20.] Bresler, B., Scordelis, A.C. Shear strength of reinforced concrete beams. In Journal Proceedings 60(1963) 51-74.

[21.] Rajagopalan, K.S., Ferguson, P.M. Exploratory Shear Tests Emphasizing Percentage of Longitudinal Steel. ACI Journal (1968)634-638.

[22.] ASCE-ACI Committee 426. The shear strength of reinforced concrete members. J. Struct. Div., ASCE 99 (1973)1091-1187.

[23.] Walraven, J.C., Reinhardt, H.W. Concrete mechanics. Part A: Theory and experiments on the mechanical behavior of cracks in plain and reinforced concrete subjected to shear loading. Nasa Sti/recon Technical Report N 82(1981) 25417.

[24.] New Zealand standard code of practice for general structural design and design loadings for buildings, Standards Association of New Zealand, (1984).

[25.] Mphonde, A. G., Frantz, G.C. Shear Tests of High-and-Low Strength Concrete Beams Without Stirrups. ACI Journal, Proceedings 81(1984)330-341.

[26.] Norwegian Standard, NS 3473 E (English Translation). Concrete Structures, Design Rules. Norwegian Council for Building, Standardization, Oslo, Norway (1989) 79.

[27.] AASHTO American Association of State Highway and Transportation Officials, LFRD Bridge design specifications (1994).

[28.] Collins, M.P., Kuchma, D. How safe are our large, lightly reinforced, concrete beams. Slabs,and footings?, ACI Struct J. 96 (1999) 482–490.

[29.] BAEL. Règles Techniques de Conception et de Calcul des Ouvrages et Constructions en Béton Armé suivant la Méthode des Etats Limites, Deuxième Edition 2000, Editions Eyrolles, Paris (1999).

[30.] Khuntia, M., Stojadinovic, B., Goel, S.C. Shear strength of normal and high-strength fiber reinforced concrete beams without stirrups. Structural Journal 96 (1999) 282-289.

[31.] TS500; TS500 Requirements for Design and Construction of Reinforced Concrete Structures. Turkish Standards Institute: Ankara, Turkey, (2000) (In Turkish)

[32.] Chinese Standard, JGJ 138-2001. Technical Specification for Steel Reinforced Concrete Composite Structures, China Building Industry Press, Beijing, (2002).

[33.] Desai, S.B. Influence of constituents of concrete on its tensile strength and shear strength. Structural Journal 101 (2004) 29-38.

[34.] Chinese Standard, YB 9082-2006, Technical Specification of Steel-Reinforced Concrete Structures, Metallurgy Industry Press, Beijing, (2007).

[35.] ISIS Canada Corporation. ISIS design manual: reinforcing concrete structures with fiber reinforced polymers-design manual No. 3. Manitoba, Canada: (2007).

[36.] Arslan, G. Shear strength of reinforced concrete beams with stirrups. Materials and Structures 41(2008) 113-122.

[37.] Ministry of land, transport and maritime affairs Korean Building Code (KBC) Arch institute of Korea, Seoul (2009).

[38.] AISC 360-10, Specification for Structural Steel Buildings, American Institute of Steel Construction, Chicago, Illinois, (2010).

[39.] GB50010-2010 Ministry of Housing and Urban Rural Development of the People's Republic of China. Code for Design of Concrete Structures; China Architecture & Building Press: Beijing, China, (2011).

[40.] CEB-FIP Model Code 2010 Volume 2 – Final Draft Bulletin 66, International Federation for Structural Concrete (fib), (2012).

[41.] Associação Brasileira de Normas Técnicas, Projeto de Estruturas de Concreto-Procedimento, NBR 6118, (2014).

[42.] Egyptian code for design and construction of reinforced concrete structures (ECP 203–2017), (2017).

[43.] Rahal, KN, and YT Alrefaei. Shear Strength of Longitudinally Reinforced Recycled Aggregate Concrete Beams. Engineering Structures 145 (2017)273-82.

[44.] Etman, E.E., Afefy, H.M., Baraghith, A.T. Khedr, S.A. Improving the shear performance of reinforced concrete beams made of recycled coarse aggregate. Construction and Building Materials 185 (2018) 310-324.

[45.] Canadian Standards Association (CSA), Design of Concrete Structures, A23.3- 19, Canadian Standards Association, Ottawa, Canada, (2019).

[46.] Okamura H, Higai T. Proposed design equation for shear strength of reinforced concrete beams without web reinforcement. Proceedings of the Japan Society of Civil Engineers. 300 (1980)131-41.

[47.] Mansur, M.A., Ong, K.C.G., Paramasivam, P. Shear strength of fibrous concrete beams without stirrups. Journal of structural engineering, 112 (1986) 2066-2079.

[48.] Hedman, O.; Losberg. A. Design of concrete structures with regard to shear forces. CEB Bulletin 126, (1978).

[49.] Mphonde, A. G., Frantz, G. C. Shear Tests of High-and Low-Strength Concrete Beams with Stirrups," ACI SP 87.10 on High Strength Concrete (1985) 179-196.

[50.] Kumar, P., 1976. Collapse load of deep reinforced concrete beams. Magazine of concrete Research 28 (1976)30-36.

[51.] Bazant Z. P., Planas, J. Fracture and size effect in concrete and other quasibrittle materials. Routledge (2019). Teng, G., Hu, Y.M., Behaviour of FRP-jacketed circular steel tubes and cylindrical shells under axial compression. Construction and Building Materials 21 (2007) 827–838.

How to Cite This Article

Abdulla, N. A., Concrete's Role in Plain Concrete Deep Beams' Shear Strength, Brilliant Engineering, 2(2026), 41109.
https://doi.org/10.36937/ben.2026.41109